



POLİTEKNİK DERGİSİ

JOURNAL of POLYTECHNIC

ISSN: 1302-0900 (PRINT), ISSN: 2147-9429 (ONLINE)

URL: <http://dergipark.org.tr/politeknik>



Optimization of plenum for control of boundary layer-shock interaction in supersonic inlet

Ses üstü hava alığında sınır tabaka - şok etkileşiminin plenum optimizasyonu ile kontrolü

Yazar(lar) (Author(s)): Zeliha TÜRKKAHRAMAN, Muhammed Enes ÖZCAN, Buğrahan ALABAŞ³

ORCID¹: 0000-0001-9517-3219

ORCID²: 0000-0002-1171-3749

ORCID³: 0000-0002-1040-1110

To cite to this article: Türkkahraman Z., Özcan M. E. and Alabaş B., “Optimization of Plenum for Control of Boundary Layer-Shock Interaction in Supersonic Inlet”, *Journal of Polytechnic*, 27(4): 1269-1279, (2024).

Bu makaleye şu şekild atıfya bulunabilirsiniz: Türkkahraman Z., Özcan M. E. and Alabaş B., “Optimization of Plenum for Control of Boundary Layer-Shock Interaction in Supersonic Inlet”, *Journal of Polytechnic*, 27(4): 1269-1279, (2024).

Erişim linki (To link to this article): <http://dergipark.org.tr/politeknik/archive>

DOI: 10.2339/politeknik.1247300

Optimization of Plenum for Control of Boundary Layer-Shock Interaction in Supersonic Inlet

Highlights

- ❖ A reference supersonic inlet has been numerically validated.
- ❖ Plenum design was made and its effect on pressure recovery was examined.
- ❖ Pressure recovery was improved by optimizing the plenum geometry.

Graphical Abstract

In this study, a plenum design was made for supersonic air intake and it was optimized. The effect of optimized geometry on pressure recovery and flow distortion was investigated.

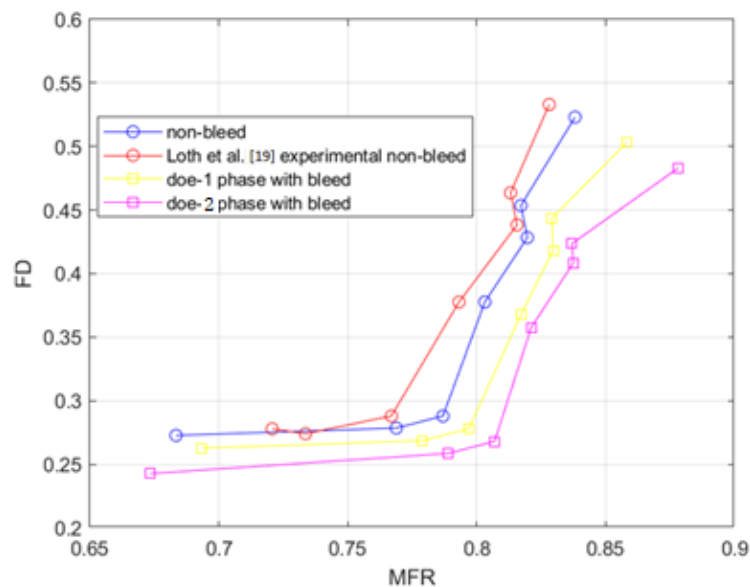


Figure. 21

Aim

In this study, it is aimed to increase the pressure recovery in the supersonic air inlet by the design and optimization of the plenum.

Design & Methodology

An optimization process has been applied to improve the aerodynamic performance of the supersonic air inlet. Optimum geometry was determined by inserting different geometries into CFD analysis.

Originality

In this study, a original geometry optimized for a supersonic air intake was determined by making a special plenum design.

Findings

It has been observed that the bleed hole diameter and the angle it makes with the air inlet channel directly affect the performance criteria.

Conclusion

The optimized new geometry has been found to have high pressure recovery and low flow distortion.

Declaration of Ethical Standards

The author(s) of this article declare that the materials and methods used in this study do not require ethical committee permission and/or legal-special permission.

Optimization of Plenum for Control of Boundary Layer-Shock Interaction in Supersonic Inlet

Research Article

Zeliha TÜRKKAHRAMAN^{1*}, Muhammed Enes ÖZCAN², Buğrahan ALABAŞ³

¹ Department of Aeronautical Engineering, Faculty of Aeronautics and Astronautics, Erciyes University, Turkey

² Turkish Aerospace Industries Inc. 06560, Ankara, Turkey

³ Department of Aeronautical Engineering, Faculty of Aeronautics and Astronautics, Erciyes University, Turkey

(Received : 11.02.2023 ; Accepted : 12.04.2023 ; Early View : 04.06.2023)

ABSTRACT

In the developing world, the importance of supersonic flights is increasing day by day, especially in military fields. Since supersonic flights have different physical conditions, different designs are required both in the fuselage structure and in the engine part compared to subsonic aircraft. In these studies, the air inlet performance of jet engines designed for supersonic flights is investigated. A plenum has been added to the air inlet geometry in line with the goal of low flow distortion and high pressure recovery. Then, the optimum plenum geometry design was obtained by applying a two-stage optimization process. In each optimization step, computational fluid dynamics analyses were performed to define the effects of the changes in the geometric dimensions of the plenum design and bleed system on the PR (Pressure Recovery) and FD (Flow Distortion) values. The outcome of the analysis showed that the addition of the plenum and the bleed system improved the performance of the air inlet. The new plenum design that emerged as a result of the optimization processes has positively affected the performance values of the air intake. Analysis results showed higher PR and lower FD results in optimized geometry.

Keywords: Supersonic Air Inlet, Optimization, Pressure Recovery

Ses Üstü Hava Alışında Sınır Tabaka – Şok Etkileşiminin Plenum Optimizasyonu ile Kontrolü

ÖZ

Gelişen dünyada özellikle askeri alanlarda süpersonik uçuşların önemi her geçen gün artmaktadır. Ses üstü uçuşlar farklı fiziki şartlara sahip olduğundan ses altı uçaklara göre hem gövde yapısında hem de motor kısmında farklı tasarımlar gerekmektedir. Bu çalışmalarda süpersonik uçuşlar için tasarlanmış jet motorlarının hava giriş performansları araştırılmaktadır. Yüksek basınç geri kazanımı ve düşük akış distorsiyonu hedefine uygun olarak hava giriş geometrisine plenum eklenmiş ve iki aşamalı optimizasyon süreci uygulanarak optimum plenum geometri tasarımı elde edilmiştir. Her bir optimizasyon adımında, plenum tasarımı ve tahliye sisteminin geometrik boyutlarındaki değişikliklerin PR (Basınç Geri Kazanımı) ve FD (Akış Bozulması) değerleri üzerindeki etkilerini belirlemek için hesaplamalı akışkanlar dinamiği analizleri yapılmıştır. Yapılan analiz sonucunda plenum eklentisi ve tahliye sisteminin hava giriş performansına olumlu etkisi olduğu görülmüştür. Optimizasyon süreçleri sonucunda ortaya çıkan yeni plenum tasarımı, hava emişinin performans değerlerini olumlu yönde etkilemiştir. Analiz sonuçları, optimize edilmiş geometride daha yüksek PR ve daha düşük FD sonuçları gösterdi.

Anahtar Kelimeler: Süpersonik Hava Alışı, Optimizasyon

1. INTRODUCTION

Boundary layer control in supersonic air inlet is an important issue that has been studied and developed in the field of aviation studies for years. It is a very important and critical issue to prevent flow separation due to reverse pressure gradients and boundary layer-shock interaction in this type of air inlet. The occurrence of these negative effects, firstly, radically changes the structure of the flow. Second effect, it may cause the shock wave model to be moved from the efficient configuration to the less efficient configuration. In addition, due to flow separation, the uniformity of the flow is disturbed. Flow controllers are used to prevent or

reduce the performance and efficiency degradation caused by boundary layer separation. Different flow control methods for air intakes are also applied and researched in the literature. However, the bleed system is the most preferred flow control method. Bleed design is one of the most critical considerations to ensure the overall performance required in all operating conditions of the inlet. As computer technology advances, so does the field of computational fluid dynamics (CFD), simulating and visualizing complex bleed flow events under supersonic velocity conditions have provided the opportunity and convenience to design in accordance with inlet operating conditions.

* Corresponding Author

e-mail : bugrahanalabas@erciyes.edu.tr

Zhou et al., [1] numerically modeled the interaction between the boundary layer and the shock wave in their study and verified it with experimental results. In the two-dimensional study, according to the simulation data, the flow separation length was analyzed between 2 and 7 Mach numbers, where the strength of the shock wave is dependent on the Mach number and Reynolds number. Two different models have been proposed for low and high mach numbers for the estimation of the SWBLI (Shock wave/Boundary Layer Interaction) split length. Choe et al. [2] conducted research to determine the impact of an optimized bleed system on the performance of a supersonic air inlet. In the study, analyzes were performed under different plenum inlet pressure, location, width and inlet conditions. Numerical results make visible that the bleed conditions obtained by multi-point design optimization significantly increase the overall pressure recovery. Liou and Benson [3] have optimized the bleed system for a supersonic air inlet. Total pressure recovery and total evacuated air mass were determined in the analyses. As a result of the datas obtained in the study, a genetic algorithm was added to the design process. Navier-stokes solver is proposed to increase computational efficiency. Younsi et al. [4] carried out an experimental study to assess the impact of the boundary layer bleed system and Mach number on the stability of flow in a supersonic air inlet. The findings indicated that a rise in the Mach number led to a decrease in the stability of the flow within the air inlet. Thanks to the bleed system, flow separation is prevented and a greater flow is achieved and a smaller amplitude of shock oscillations is measured during the buzz phenomenon. Abedi et al. [5] used simulation to analyze the axisymmetric and three-dimensional flow in a supersonic inlet geometry that is used for compression. The outcome of the study revealed that the total pressure distributions obtained from the simulations were in good agreement with the experimental data. This suggests that the simulation models accurately captured the behavior of the flow in the supersonic inlet geometry, and could be useful for predicting the performance of similar systems. Gnani et al., [6] investigated the interaction of pseudo-shock waves and high-speed inlet. In the study, the authors examined various flow control techniques aimed at modifying the interaction between the shock wave and boundary layer. As a result of the study, multiple flow controllers have been proposed.

Lee et al., [7] investigated the flow characteristics of a small-scale supersonic inlet. Two different models, rectangular and axisymmetric input, were tested in the study. The results indicated that the buzz phenomenon observed in the smaller inlet was comparable to that in the larger inlet. However, it was stated that the small entrance is more easily affected by the presence of the separation bubble. Younsi et al., [8] found boundary layer suction investigations for high velocity inlets. In the study, it was stated that the bleed system is intended to be used to improve the inlet performance and to reduce buzz oscillations. In addition, a comparison was made

between the effectiveness of other flow control methods and the bleed system. Ferrero, [9] also compared plasma actuators for supersonic inlet conditions in his study on the bleed system. Simulation results confirm large flow separations at large Mach numbers, while the two systems are compared in terms of total pressure recovery and power consumption. The study stated that the bleed system is known for having a minimal separation bubble in the isolator. Suryanarayana and Dubey [10] studied Passive Bleed of Boundary Layer optimization for a ramjet air inlet. The results showed that a 1.6 mm gap provided the best efficiency, although all gap structures improved overall pressure recovery and mass flow rate. Askari and Soltani [11] examined the asymmetric and symmetrical performance of a supersonic input. Experiments in the wind tunnel were carried out at Mach 1.65 at 0° angle of attack. The results showed that a symmetrical supersonic flow emerged under both supercritical and critical operating conditions.

Soltani et al. [12] examined the impact of the location of the bleed system on the stability of a supersonic inlet in their study. In the study conducted at three different Mach numbers (1.8, 2.0, 2.2), they stated that spilled normal shock can be found depending on the design and flow separation occurs at the beginning of the buzz. Maadi and Younsi [13] studied the impact of the type of bleed on the performance of a supersonic air intake in their research. The study results showed that the porous bleed structure increased the total pressure recovery under all experimental conditions. In addition, lower flow distortion occurred in the porous bleed structure compared to the slot bleed structure. Suryanarayana et al. [14] explored the nonlinear damping model for the buzz phenomenon in a supersonic air intake in their study. In the study performed under Mach number 3 conditions, shock oscillation was observed using a high-speed camera. A dominant relationship was found between shock oscillations and a frequency of 103.8 Hz. Abedi et al., [15] numerically investigated the formation of buzz in a supersonic air intake. Buzz formation is an unstable and self-sustaining feature under subcritical operating conditions. The results show that the conical and lambda shocks occurring in the compression ramp cause the flow to move upward. In addition, it has been observed that both the total pressure and the static pressure peaks and troughs are directly related to the buzz amplitude.

Herrmann and Gulhan [16] experimentally tested a bleed system for the air inlet section of a missile. The study was carried out between 2.5 – 3.5 Mach numbers. The results showed that the efficiency of the bleed system is dependent on flow instabilities and flow separations. Titchener and Babinsky [17] used a combined vortex generator and bleed system to control the interaction of shock waves in supersonic flow with the boundary layer. The results showed that flow improvement occurs when flow control is applied. It has also been observed that the vortex generator can be effective in reducing the need for boundary layer bleed. Ryu et al., [18] investigated the effect of attack angle change on bleed system

performance. The feature of this study is that it is done in a double cone type air intake. The results showed that the bleed system successfully discharged the low energy flow. In addition, with the increase in the angle of attack, uneven flow areas were seen in the Aerodynamic Interface Plane.

The literature review clearly demonstrates the importance of controlling the boundary layer/shock wave interaction. In studies where different flow control devices are used, it has been seen that the bleed system is still the most advantageous system. In contrast to previous studies in the field, plenum design with a narrowing section that can evacuate air with higher pressure by occupying less space was made. First, the reference experimental study was validated for different EFM (Engine Face Mach Number) values in a double ramp supersonic air inlet. The study, which was carried out with CFD (Computational Fluid Dynamics) methods, was carried out in 2D. In similar studies in the literature, since the two-dimensional analyzes were of sufficient accuracy and 3D analyzes were not the most appropriate choice, two-dimensional analysis was preferred in this study as it was seen that [5]. By observing the PR (Pressure Recovery) and FD (Flow Distortion) performance effects, a DOE (Desing of Experimental) study was conducted to optimize the most appropriate plenum measures. CFD analysis was performed again to examine the effect of each change by making changes in the plenum geometry in the DOE studies. Optimized geometry for the DOE process was found for two different configurations and performance evaluation was made according to the first situation. The most important difference of this study from those in the literature is that a new plenum design is subjected to the optimization process through statistical data analysis. In this way, the plenum design and bleed system, which will achieve the highest performance, will be determined and the deficiencies in the literature will be covered.

2. NUMERICAL SETUP

Figure 1 shows the scaled form of the numerically modeled supersonic inlet. The capture height in the air intake used in the reference experimental study was determined as 22 mm [19]. Different domains are assigned in order to mesh more frequently to potential shock regions that will occur during flow. Complex flow can be observed in the boundary layer, such as flow separation. In this context, it is necessary to model the boundary layer formed on the air inlet walls. In order to observe this complex behavior well, the number of cells increases due to the dense mesh applied to those parts. In order to accurately model the mesh, the boundary layer thickness must be known. Since the system has double ramps, instead of calculating numerically, a high mesh is thrown into that area as much as possible and the boundary layer thickness is calculated as approximately 1.9 mm as a result of the analysis. In order for the turbulence model to be used to adapt well to the boundary, more accurate modeling and a more accurate result, $y^+ = 1$ is taken. As a result, the first cell height was

found to be 0.001 mm. In the inlet geometry used in the study, according to the free flow direction, there is a first ramp with 8° from the upper part of the inlet and a second ramp with 15° . The Mach number is chosen as 2 in the inlet conditions, it decreases to Mach 1.7 with the first oblique shock, and down to Mach 1.4 after the second oblique shock wave. After the normal shock, it decreased to Mach 0.7 and reached Mach 0.48 in the AIP region with the difusser effect. The free flow stagnation pressure was chosen as 61.7 kPa, and the stagnation temperature was 339 K.

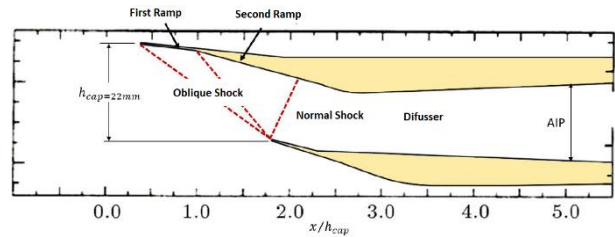


Figure 1. Scaled Air Intake [19]

A mesh element size of 4 mm was applied in the outer area. The mesh density increases in the inner open part. A mesh element size of 0.8 mm is used in the internal flow domain. There are oblique and normal shocks in the potential shock region. The highest mesh density was applied to this region because the shock wave caused large changes in the flow. The mesh element size of the potential shock zone is 0.2 mm. The mesh structure density changes are shown in Figure 3. In order not to deteriorate the mesh structure and to give more accurate results, radius are given to the corners of the air intake wall. The radius of the cowl lip and the head of the ramp was determined as 0.1 mm in order not to deteriorate the shock structure. In Figure 2.c, the corner fillet part is presented in detail.

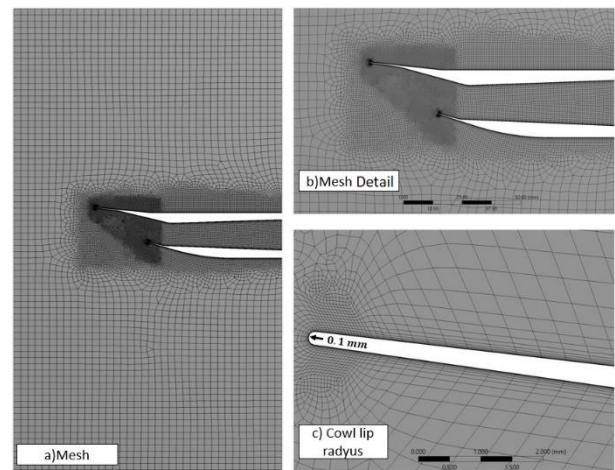


Figure 2. Mesh Structure

In this study, the realizable $k-\epsilon$ model was used as the CFD turbulence model. In the literature, it is stated that the standard $k-\epsilon$ model and other conventional models have weak ability to validate the experimental results in axisymmetric jet flows. This model is an improvement of the standard model, includes the effect of different

turbulent viscosity in the formula. This model gives more accurate results for separated flows and complex flows, especially in regions close to the boundary layer. Equation 1 shows turbulent viscosity calculation. In addition, the calculations used in the numerical model are presented in equations 2-7. In equations; (k) is the kinetic energy of the turbulent, (ε) is the turbulent damping ratio. In this way, the turbulent length and velocity scale was determined [20,21]. It is seen that the CFD method is frequently used in aerodynamic studies [22,23,24].

$$\mu_t = \rho c_\mu V_t l_t \tag{1}$$

$$V_t = \sqrt{k} \tag{2}$$

$$l_t = \frac{k^{\frac{3}{2}}}{\epsilon} \tag{3}$$

$$\mu_t = c_\mu \frac{\rho k^2}{\epsilon} \tag{4}$$

Convection equation for turbulent kinetic energy (k):

$$\frac{\partial(\rho k)}{\partial t} + \nabla \cdot (\rho U k) = \nabla \cdot \left[\left(\mu + \frac{\mu_t}{\sigma_k} \right) \nabla k \right] + P_k + P_b - \rho \epsilon + S_k \tag{5}$$

Convection equation for turbulent damping ratio(ε):

$$\frac{\partial(\rho \epsilon)}{\partial t} + \nabla \cdot (\rho U \epsilon) = \nabla \cdot \left[\left(\mu + \frac{\mu_t}{\sigma_\epsilon} \right) \nabla \epsilon \right] + C_1 \frac{\epsilon}{k} (P_k + C_3 P_b) - C_2 \rho \frac{\epsilon^2}{k} + S_\epsilon \tag{6}$$

3. RESULT and DISCUSSION

3.1. Mesh Independence and Validation of Experimental Study

First of all, it is necessary to determine the accuracy of the calculations for the air inlet analyzed in the numerical study, and its mesh independence has done. It is known that as the mesh size decreases, the accuracy of the solution will increase. On the other hand, with the increasing number of meshes, the time and cost required to make calculations will increase. Increasing the number of elements after the mesh element number reaches a value will not change the accuracy of the solution. Therefore, the minimum network structure that the solution will reach ideal accuracy should be determined. Figure 3 shows the distribution of Total pressure ratio along the dimensionless height in AIP. The total pressure ratio is found by dividing the total pressure at the AIP by the free flow total pressure. As a result of the study, it was seen that sufficient accuracy was achieved with the number of cells reaching 20000 in the air inlet geometry taken from the literature.

In Figure 4, previous studies on the reference air intake and the data of this study are compared. In the comparison, the data of the total pressure ratio distribution along the height of the AIP were taken into account. When the results are examined, it is seen that this study gives very close results to the reference

experimental study [19] compared to previous numerical studies. While the standard k-ε model was used in previous numerical studies, the use of the realizable k-ε model in this study increased the accuracy of the results.

In the reference study, it was observed that the oblique shock, normal shock and lambda shock structure occurred on the ramps inside the air inlet and at the last entrance. Since a similar shock structure will occur in this study, mesh modification was made especially in this region. As a result of the mesh modification, oblique shock, normal shock and lambda shock structures were seen more clearly. Changes in the flow due to these shocks were detected more accurately. Figure 5 shows the Mesh modification of the current study. In addition, in Figure 6, the density gradient in this study is compared with the reference study of Loth et al [19]. Shock structures were captured similarly and the study was confirmed in terms of intensity gradient.

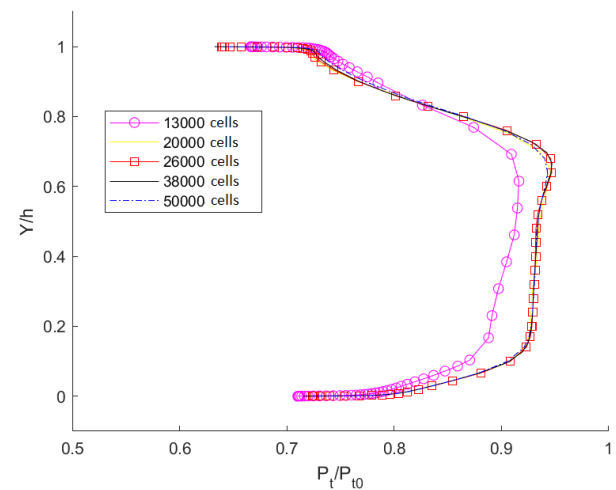


Figure 3. Total pressure ratio distribution along the height of the AIP

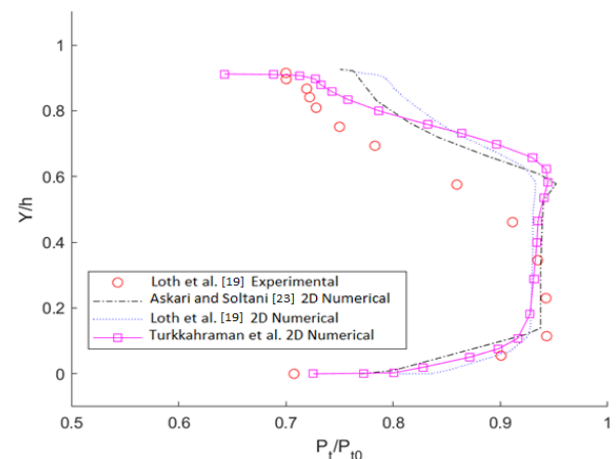


Figure 4. Comparison of the total pressure ratio distribution along the height of the AIP

In both the reference study and the current study, the air is compressed as from the outside. It means that any shock wave is observed after the lip section. Before the

lip section, two oblique shocks are obtained by using two different ramps. Ramps are used to increase overall pressure recovery. Total pressure recovery mathematically means the ratio of the total pressure in the AIP to the free flow total pressure. This term means the capacity of air to do work. A low pressure recovery means that a lot of energy is lost as the air reaches the AIP [25]. As is known from the classical supersonic flow rules, the presence of an oblique shock wave before the normal shock reduces the entropy increase and the total pressure loss. An increase in the number of ramps increases pressure recovery, but adds complexity and weight in the inlet geometry.

In Figure 7, the dimensionless static pressure can be seen relative to the dimensionless x-direction location on the inner bottom wall of the trough. The static pressure is made dimensionless by proportioning the free flow total pressure, and the x-direction position is made dimensionless using the capture height. As seen in Figure 7, the current new numerical simulation showed better accuracy than the numerical simulation of Askari and Soltani [26] and gave results closer to the experimental data in the reference study.

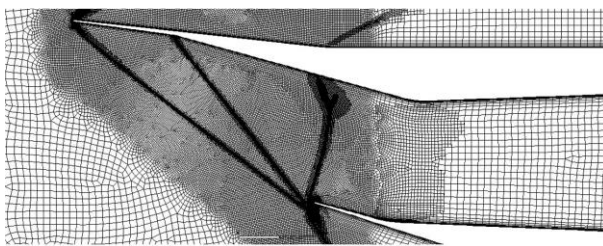


Figure 5. Current working mesh modification

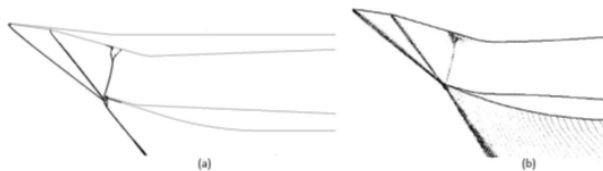


Figure 6. Density gradient (a) Current study vs. (b) Reference study [19]

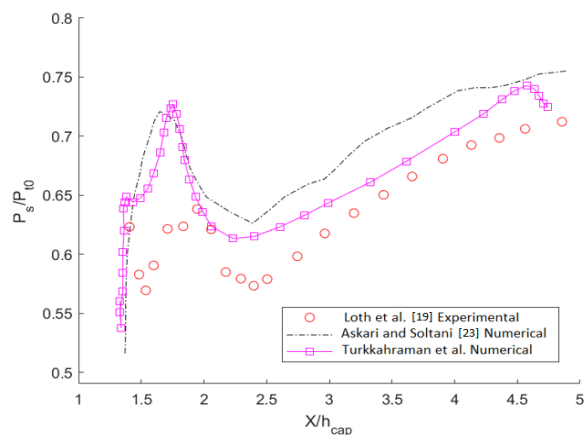


Figure 7. Dimensionless static pressure ratio relative to the dimensionless x-direction position on the air inlet inner bottom wall

In this part of the study, the validation of the numerically obtained data was completed. Three different parameters were verified with the distribution of the total pressure ratio along the height of the AIP, the location and type of shock waves in the air inlet. The verification with three different parameters proves that the changes to be made in the next part of the study and its effect on pressure recovery are interpreted according to the correct numerical results.

3.2. Desing of Plenum

Interactions between shock waves and turbulent boundary layers along the air intake geometry can lead to flow separation in the boundary layer. This can cause performance degradation and propulsion system instability. One option is to locate bleed zones on air inlet surfaces to mitigate the negative effects of shock/boundary layer interactions. In this design, the bleed system is implemented by creating holes in the surfaces that allow a portion of the air intake core flow to be removed. The holes are typically arranged in bands or sequential groups. As the air passes through the bleed system, it moves into the plenum section with a lower static pressure. The purpose of the bleed system is to regulate the flow of air in the air intake and improve its overall performance. The flow thrown by the bleed system is generally low momentum flow [27]. In this way, a higher momentum boundary layer remains, reducing the possibility of flow separation. In this part of the study, Bleed system and Plenum design will be made on the air intake geometry verified in the previous section. Then, DOE (Desing of Experiment) study will be done in order to obtain the optimum geometry.

First of all, numerical analysis was performed between $EFM = 0.1 - 0.8$ values with 0.05 value increments in order to see that the bleed system designed for air inlet works correctly and to determine the subcritical, critical and supercritical EFM (Engine Face Mach Number) values. These analysis results were compared in terms of PR (Pressure Recovery) – MFR (Mass Flow Ratio). In the section where Numerical Setup was introduced, it was stated that the shock structure in the air inlet reached the desired structure at $EFM = 0.48$. In this preliminary analysis, it was determined that the critical region was between $EFM = 0.45 - 0.5$ values. In the further part of the study, the $EFM = 0.45$ value, at which the subcritical value is captured, was determined as the operating condition of the bleed system. Figure 8 shows the PR – MFR graph. The MFR value in this graph is found by the ratio of the mass flow passing through the AIP to the flow rate passing through the air inlet capture region. Figure 9 shows the change in supersonic air inlet mach number countours for $EFM = 0.45$. As the final distribution is examined, oblique shock, normal shock and lambda shock waves occurring in the air inlet are clearly visible. In addition, Mach number variation in the boundary layer region also occurs.

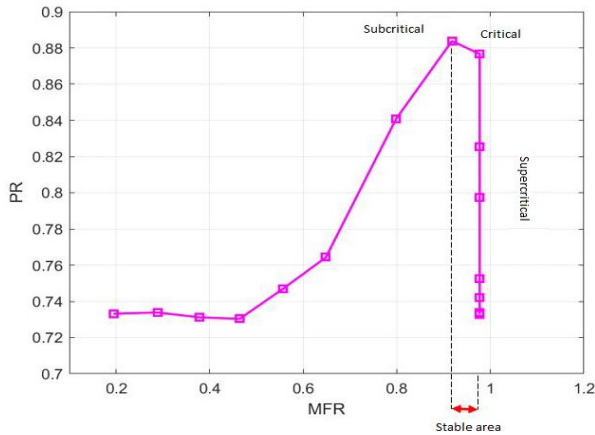


Figure 8. PR – MFR change at different EFM values

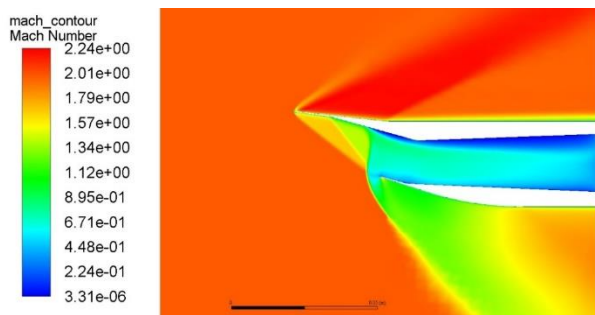


Figure 9. Contours of Mach number at EFM = 0.45

For the stability of the normal shock in the air inlet, a 30° bleed was used before the normal shock. In addition, 90° bleed was used after the normal shock, where most of the main evacuated air exited. Since the pressure dissimilarity between the main flow and the plenum is not great before the normal shock, the bleed before the normal shock is angled so that it can catch the flow [28]. Since the parameter providing the actual air outlet in the system is the plenum outlet area, this area is kept smaller than the sum of the bleed area. Figure 10 shows the bleed system and plenum specially designed for the study. All the criteria of this initial design drawn are non-standard. After the first DOE (Desing of Experimental) process, the draft dimensions will be clear. Then, with the first stage, the optimized geometry will be determined by going through a two stages of DOE (Desing of Experimental).

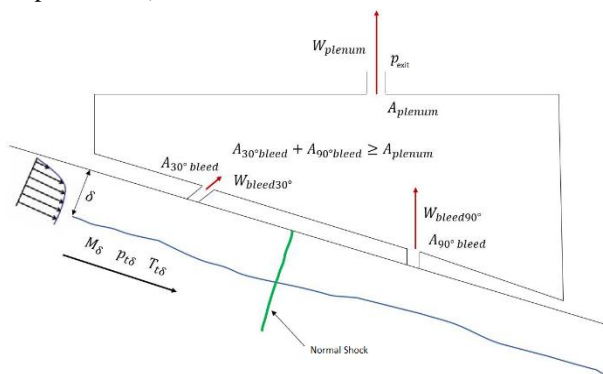


Figure 10. Bleed and Plenum schematic representation

3.3.Desing Optimization

DOE (Desing of Experimental) is a method that helps you to simultaneously investigate the effects of input variables on an output variable [29]. In this study, full factorial option from DOE methods is used for design optimization and determination of final parameter values. In the full factorial option, the effect of all factors and their interaction on the results is investigated. Creates experimental points using all major combinations of factor levels in each trial or repetition of experiments. By looking at the effect of the factors on the performance parameters, the option that gave the best result was used in the next configuration, and the effect of the new parameters determined in that configuration was examined. In this way, as a result of iterative DOE operation with different parameters, the best configuration creates the final topology of the plenum and bleed geometry. The full factorial design method was used for the optimization of all analyzes. For Configuration 1, a two-level five-factor statistical dataset was created with a full factorial design. The expression we define with the name "Level" is the values that a factor or parameter can take and corresponds to the minimum and maximum test points in full factorial design. For a two-level five-factor full factorial design, a data set requiring $2^5 = 32$ analyzes was created. Another important definition used in the optimization process is the p-value. This value expresses the effect of a variable on the analysis result, if the p-value is higher than 0.05, it indicates that the null hypothesis is valid and the variable parameter does not have a significant effect on the result. P value less than 0.05 indicates that the variable parameter is important for the result. While performing the optimization processes depending on each other, the values that have no effect were eliminated and the optimum geometry was determined. Optimized geometry was determined after the two-stage DOE process. Then, the first designed and optimized geometries were analyzed in terms of PR and FD values.

3.3.1. DOE – 1

At this stage of the study, full factorial design analysis was performed for the five parameters determined in general terms, and the effects of these parameters and their possible combinations on the performance parameters determined as PR, FD and MFR were investigated. After determining this, the final measurements were obtained from the design function in order to get an objective result, especially giving high PR and low FD values. With the increase in the number of parameters, the size of the statistical data set also increases as an exponential function. For this, as a result of the analyzes made for each configuration, the values of the parameters that have the main effect on the performance data were determined functionally to be

used in the next configuration. In this way, the final bleed and plenum geometry was determined in relatively less time. In Figure 11, the variables to be optimized are presented on the plenum geometry. The length L1 shown in the figure represents the distance of the plenum outlet from the narrow section, L2 the diameter of the plenum outlet, L3 the distance of the bleed hole positioned at 30° from the narrow section, L4 the 30° angle bleed diameter, and L5 the 90° angle bleed diameter.

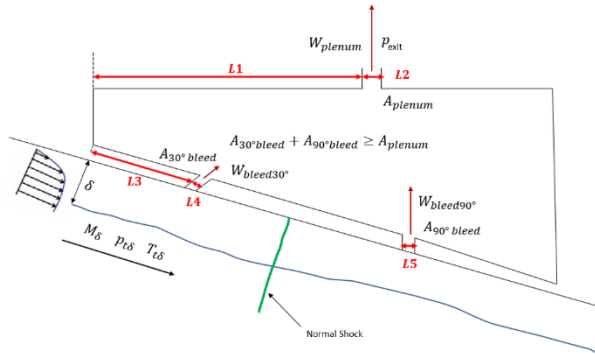


Figure 11. Parameters to be optimized in DOE – 1 phase

In Figure 12.a, the effect of five parameters determined as variables on the PR (Pressure Recovery) value is presented. The fact that the p-value is below 0.05 in the results means that the effect of the variable on the result is high. If this value is above 0.05, it means that the effect of the determined parameter on the result is insignificant and the null hypothesis is realized. According to the result, it is seen that the parameters that have the main effect on the PR value are the plenum outlet diameter indicated by L2 and the bleed diameter of 90° after the normal shock, defined as L5. When Figure 13.a is examined, the PR values between the maximum and minimum points of five different parameters are shown. As can be seen from this graph, it is seen that L2 and L5 variables have the main effect on PR. When the effect on the FD value in case of change of the same parameters in Figure 12.b is examined, it is seen that while the lengths of L2 and L5 are similarly effective, the distance from the narrow section of the plenum exit expressed as L1 is also effective. In Figure 13.b, the FD change for all length values is presented. It is seen as an advantageous situation that the increase in L1, L2 and L5 values is FD (Flow Distortion), the flow is more smooth and the distortion is reduced. The reason why the L5 value is important is that it is placed after the shock wave that causes flow separation. The diameter of this hole, as well as the diameter of the plenum outlet, is of high importance for the discharge of low-energy flow.

Term	P-Value	Term	P-Value
Constant	0,000	Constant	0,000
L1	0,110	L1	0,009
L2	0,000	L2	0,000
L3	0,281	L3	0,266
L4	0,138	L4	0,573
L5	0,000	L5	0,000

Figure 12. P-values of variables determined for DOE-1 a) PR, b) FD

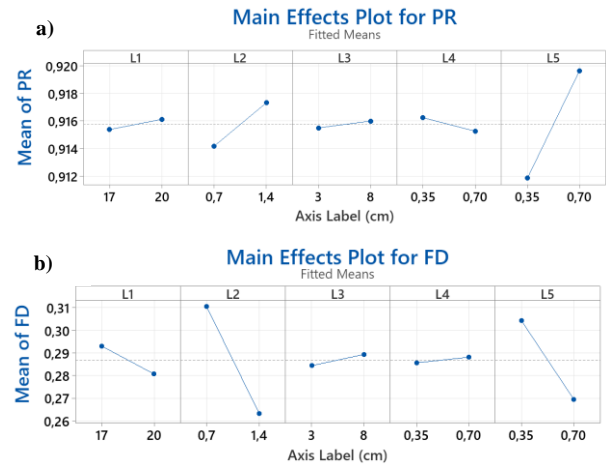


Figure 13. The effect of variables determined for DOE-1 on a) PR, b) FD change

As a result of the first stage of the design of experimental processes, optimized results were determined. Figure 14 presents the results. According to these results, while the pressure recovery is expected to be maximum for an efficient engine operation, the condition of minimum flow distortion is sought. As a result, L1 (distance of plenum outlet from narrow section) = 20 cm, L2 (plenum outlet diameter) = 1.4 cm, L3 (distance of bleed hole positioned at 30° from narrow section) = 3 cm, L4 (bleed diameter at 30° angle) = 0.35 cm, L5 (90° angled bleed diameter) = 0.7 cm. It has been determined that a design made according to these dimensions is a more advantageous geometry for PR and FD values among the options. The large bleed diameter caused the low-energy flow that emerged after the shock wave to be quickly evacuated from the air inlet. In addition, increasing the plenum outlet diameter similarly increased the system efficiency.

Parameters

Response	Goal	Lower	Target	Upper
FD	Minimum		0,231279	0,338401
PR	Maximum	0,909389	0,922290	

Solution

Solution	L1	L2	L3	L4	L5	FD Fit	PR Fit	Composite Desirability
1	20	1,4	3	0,35	0,7	0,235789	0,921842	0,961575

Figure 14. Results of Optimization (DOE – 1)

The bleed system and plenum were redesigned and subjected to CFD analysis according to the length

measurements resulting from DOE-1. When the Mach Contour situation presented in Figure 15 is examined, the 30° bleed positioned before the normal shock disrupts the shock structure in the flow. In addition, since the bleed positioned after the normal shock could not absorb enough air, the low-momentum part of the boundary layer could not be completely withdrawn in the part of the second ramp after the normal shock. This can be easily understood from the color change in the figure. Although the results showed that the geometry that emerged as a result of the first optimization was effective in increasing the PR value and reducing the FD size, the DOE process was performed again to reveal the more optimum bleed system and plenum design due to the deterioration in the flow.

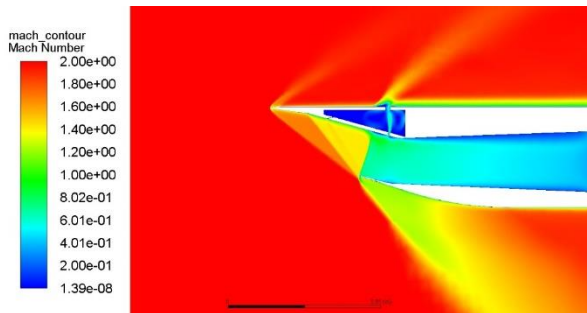


Figure 15. DOE – 1 Optimization result Mach Contour

3.3.2.DOE – 2

Finally, in the optimization part of the study, many optimized parameters were re-evaluated both on their own and in their interactions with each other, and the second optimization process was carried out. At this stage, D1 presented in Figure 16 shows the plenum outlet diameter, while D2 represents the bleed diameter. While the α angle was again optimized as the bleed angle, the bleed length L expression was also included in the final optimization. In this way, it is aimed to obtain the optimum design by examining the effect of bleed length on the other three variables. Three parameters, which were found to have a significant effect on the changes in FD and PR values in the previous three optimization stages, were also re-evaluated in the final optimization stage. As a result, a two-level four-factor data set should be created using the full factorial design method. As a result of the expression 24, all parameters and their possible combined effects were investigated as a result of the data set with 16 analyzes.

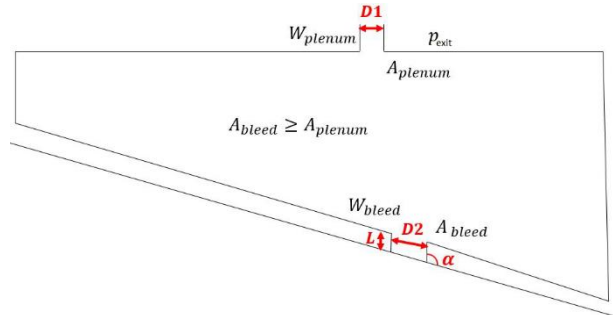
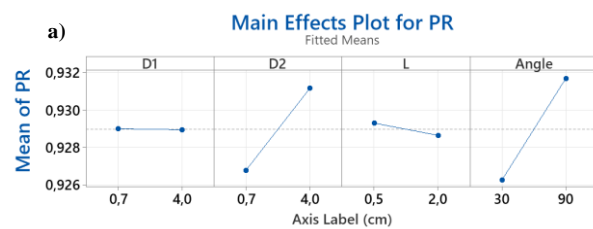


Figure 16. Parameters to be optimized in DOE – 2 phase

The p-value data that emerged in the analyzes performed within the scope of DOE-2 are shown in Figure 17. Analysis results showed that bleed diameter and angle are much more important than other parameters. It has been revealed that the bleed diameter and angle are two extremely important parameters for drawing in enough low-energy air. These two variables caused significant changes in both PR and FD values. When the PR and FD results in Figure 18 are examined, it is seen that the increase in the bleed diameter increases the pressure recovery. Maximum pressure recovery was obtained when the bleed diameter was increased to 4 cm. However, when the change in FD (Flow Distortion) value is considered, it is seen that the increase in the bleed diameter increases the FD value. Although a positive situation emerged for PR, it caused a negative effect for FD value. On the other hand, when the angle of the bleed hole with the air inlet section is increased from 30° to 90°, the maximum pressure recovery value is determined again. The increase in the angle value also caused a decrease in the FD value. As a result, the bleed angle being 90° revealed an optimum result for the air intake design.

a) Term	P-Value	b) Term	P-Value
Constant	0,000	Constant	0,000
D1	0,007	D1	0,972
D2	0,545	D2	0,014
L	0,917	L	0,671
Angle	0,049	Angle	0,004

Figure 17. P-values of variables determined for DOE-4 a) PR, b) FD



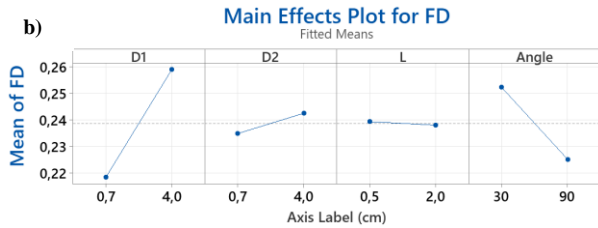


Figure 18. The effect of variables determined for DOE-2 on a) PR, b) FD change

The analysis results were evaluated together with the previous DOE stages and the optimum bleed design was revealed. According to the data presented in Figure 19, while the maximum magnitude is taken into account for the PR value, the minimum value is expected for the FD. According to the results of the analysis, it was determined that the plenum outlet diameter $D1 = 0.7$ cm and the bleed diameter $D2 = 3.51$ cm as optimum. Under these conditions, while the bleed length was $L = 0.5$ cm, 90° was determined as the bleed angle. We can see in Figure 20 how much air it draws in order to examine the performance of the optimized new plenum. As can be seen, the low-energy flow that emerged after the shock wave was largely evacuated, and the low-energy flow that could occur after the bleed was completely reduced.

Parameters

Response	Goal	Lower	Target	Upper
PR	Maximum	0,920914	0,933585	
FD	Minimum		0,175631	0,294557

Solution

Solution	D1	D2	L	Angle	FD Fit	PR Fit	Composite Desirability
1	0,7	3,51871	0,5	90	0,208030	0,932513	0,828559

Figure 19. Results of Optimization (DOE – 2)

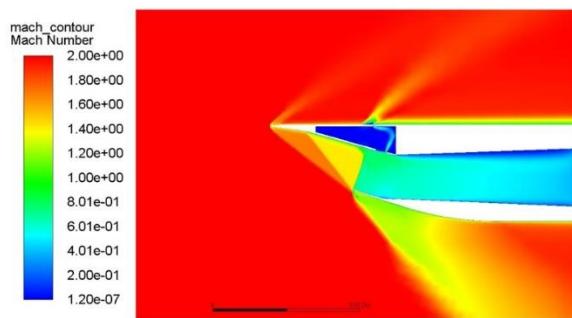


Figure 20. DOE – 2 Optimization result Mach Contour

3.4. Analysis Results of Final Geometry

As a result of the two-stage DOE performed in this study, the optimum bleed design was revealed. In Figure 21, a pressure recovery comparison is made between the reference supersonic air intake without the bleed system, the non-optimized bleed system and the air intakes using the optimized bleed system after the two-stage DOE process. In the analyzes performed at different MFR values, it was clearly seen that the use of optimized bleed

system provides high pressure recovery at all MFR values. Similarly, in Figure 22, the situation where there is no bleed system, the unoptimized bleed system and the effect of the design resulting from the optimization on the FD value are presented. As can be seen from this figure, the optimized and redesigned bleed system in this study revealed the lowest FD value.

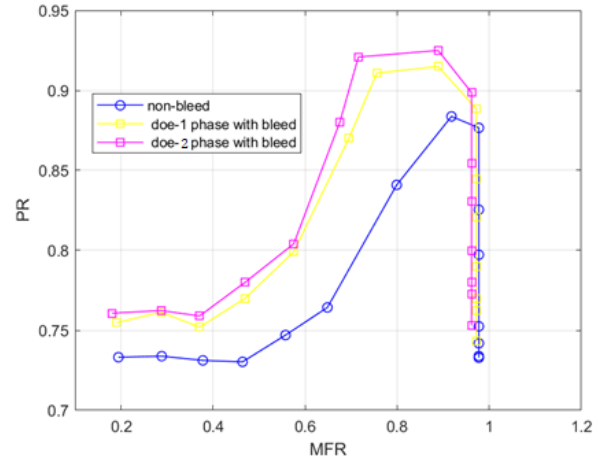


Figure 21. PR value comparison without bleed, non-optimized bleed and optimized bleed at different MFR

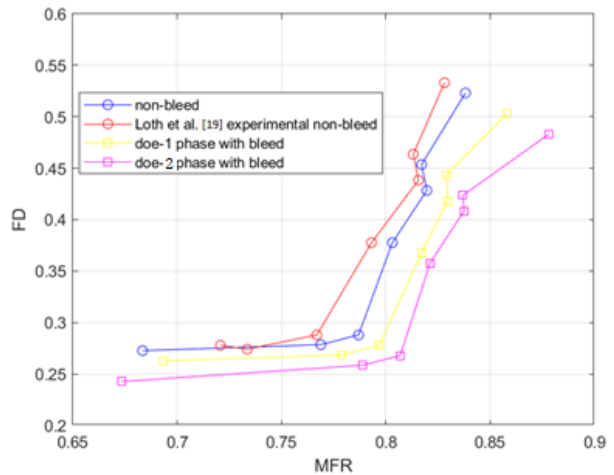


Figure 22. FD value comparison without bleed, non-optimized bleed and optimized bleed at different MFR

4. CONCLUSION

In this study, a reference supersonic air inlet geometry was verified by computational fluid dynamics method and a narrowing section plenum was designed for this air inlet. The optimized design emerged after the two-stage DOE process. Optimized bleed system design, non-optimized state and no bleed system were compared in terms of FD and PR values. The following results were obtained in the study;

- Bleed systems have been found to be efficient in preventing flow separations caused by shock waves in supersonic air vents and evacuating low energy flow regions.

- In the non-optimized bleed system design, higher PR and lower FD values were determined compared to the reference air inlet without the bleed system.
- It is considered more advantageous to place the bleed hole after the normal shock wave for efficient discharge of low energy flow.
- It has been observed that the bleed hole diameter and the angle it makes with the air inlet channel directly affect the performance criteria.
- It has been determined that the new design, which is optimized as a result of DOE processes, causes higher pressure recovery and lower flow distortion.

DECLARATION OF ETHICAL STANDARDS

The author(s) of this article declare that the materials and methods used in this study do not require ethical committee permission and/or legal-special permission.

AUTHORS' CONTRIBUTIONS

Zeliha TÜRKKAHRAMAN: Numerical analysis was carried out.

Muhammed Enes ÖZCAN: He checked the accuracy of the numerical analyzes and made suggestions.

Buğrahan ALABAŞ: Wrote the manuscript.

CONFLICT OF INTEREST

There is no conflict of interest in this study.

REFERENCES

- [1] Zhou, Y.Y., Zhao, YL., Zhao, YX. A., "Study on the Separation Length of Shock Wave/Turbulent Boundary Layer Interaction", *International Journal of Aerospace Engineering*, No. 8323787, (2019).
- [2] Choe, Y., Kim, C., Kim, K., "Effects of Optimized Bleed System on Supersonic Inlet Performance and Buzz", *Journal of Propulsion and Power*, 36(2): 1-12, (2020).
- [3] Liou, M.F., Benson, T., 2010. "Optimization of Bleed for Supersonic Inlet", *13th AIAA/ISSMO Multidisciplinary Analysis Optimization Conference*, Texas/USA, 13 – 15 Sept. 2010.
- [4] Younsi, J.S., Soltani, M.R., Abedi, M., Masdari, M., "Experimental investigation into the effects of Mach number and boundary-layer bleed on flow stability of a supersonic air intake", *Scientia Iranica*, 27(3): 1197-1205, (2020).
- [5] Abedi, M., Askari, R., Younsi, J.S., Soltani, M.R., "Axisymmetric and three-dimensional flow simulation of a mixed compression supersonic air inlet", *Propulsion and Power Research*, 9(1): 51-61, (2020).
- [6] Gnani, F., Behtash, H.Z., Kontis, K., "Pseudo-shock waves and their interactions in high-speed intakes", *Progress in Aerospace Sciences*, 82: 36-56, (2016).
- [7] Lee, H.J., Lee, B.J., Kim, S.D., Jeung, I.S., "Flow Characteristics of Small-Sized Supersonic Inlets", *Journal of Propulsion and Power*, 27(2): 306-318, (2011).
- [8] Younsi, J.S., Feshalami, B.F., Maadi, S.R., Soltani, M.R., "Boundary layer suction for high-speed air intakes: A review", *Proceedings of the Institution of Mechanical Engineers Part G Journal of Aerospace Engineering*, 233(9): 3459-3481, (2018).
- [9] Ferrero, A., 2020., "Control of a Supersonic Inlet in Off-Design Conditions with Plasma Actuators and Bleed", *Aerospace*, 7(32), (2020).
- [10] Suryanarayana, G.K., Dubey, R., "Performance Enhancement of a Ramjet Air Intake by Passive Bleed of Boundary Layer", *Journal of Spacecraft and Rockets*, 56(3): 875-886, (2019).
- [11] Askari, R., Soltani, M.R., "Symmetric and Asymmetric Performance Investigation of a Diverterless Supersonic Inlet", *AIAA Journal*, 60(4): 1-10, (2022).
- [12] Soltani, M.R., Daliri, A., Younsi, J.S., Farahani, M., "Effects of Bleed Position on the Stability of a Supersonic Inlet," *Journal of Propulsion and Power*, 32(5): 1-14, (2016).
- [13] Maadi, S.R., Younsi, J.S., "Effects of Bleed Type on the Performance of a Supersonic Intake", *Experimental Thermal and Fluid Science*, 132(9): 110568, (2022).
- [14] Suryanarayana, G.K., Singh, D.B., Surya, S., Jagadeesh, G., "Nonlinear damping model for supersonic air-intake buzz", *Aerospace Science and Technology*, 126: 107567, (2022).
- [15] Abedi, M., Askari, R., Soltani, M.R., "Numerical simulation of inlet buzz", *Aerospace Science and Technology*, 97: 105547, (2020).
- [16] Herrmann, D., Gülhan, A., "Experimental Analyses of Inlet Characteristics of an Airbreathing Missile with Boundary-Layer Bleed", *Journal of Propulsion and Power*, 31(1): 170-179, (2015).
- [17] Titchener, N., Babinsky, H., "Shock Wave/Boundary-Layer Interaction Control Using a Combination of Vortex Generators and Bleed", *AIAA Journal*, 51(5): 1221-1233, (2013).
- [18] Ryu, K.J., Lim, S., Song, D.J., "A Computational Study on the Effect of Angles of Attack on a Double-Cone Type Supersonic Inlet With Bleeding System", *Computers&Fluids*, 50(1): 72-80, (2011).
- [19] Loth, E., Roos, F., Davis, D.O., Mace, J., Jaiman, R., White, S.R., Dutton, C., 2004. "Mesoflap and Bleed Flow Control for a Mach 2 Inlet," *42nd AIAA Aerospace Sciences Meeting, Nevada*, 5 – 8 January 2004.
- [20] Shih, T.S., Liou, W.W., Shabbir, A., Yang, Z., Zhu, J., "A new k-ε eddy viscosity model for high reynolds number turbulent flows," *Computers&Fluids*, 24(3): 227-238, (1994).
- [21] ANSYS Fluent Theory Guide, ANSYS, Inc., 275 Technology Drive Canonsburg, PA 15317, November 2013.
- [22] Evran, S., Yıldır, S.Z., "NACA0009 ve NACA4415 Kanat Profillerinin Sayısal ve İstatistiksel Aerodinamik

- Performans Analizi”, *Politeknik Dergisi*, Early Access, (2023).
- [23] Selimli, S., “Yüzey Geometrisinin Mermi Aerodinamik Davranışları Üzerine Etkisinin Nümerik İncelenmesi”, *Politeknik Dergisi*, 24(1): 299-304, (2021).
- [24] Görgülü, Y.F., Özgür, M.A., Köse, R., “CFD Analysis of a Naca 0009 Aerofoil at a Low Reynolds Number”, *Politeknik Dergisi*, 24(3): 1237-1242, (2021).
- [25] Anderson, J.D., Fundamentals of aerodynamics. 6th Edition. McGraw-Hill Education, Boston, 2016.
- [26] Askari, R., Soltani, M.R., “Two and Three Dimensional Numerical Simulation of Supersonic Ramped Inlet”, *Scientia Iranica*, 25(4): 2198-220, (2018).
- [27] Slater, J. W., Saunders, J.D., “Modeling of Fixed-Exit Porous Bleed Systems for Supersonic Inlets”, *Journal of Propulsion and Power*, 26(2), (2010).
- [28] Slater J.W., “Improvements in Modeling 90-degree Bleed Holes for Supersonic Inlets,” *Journal of Propulsion and Power*, 28(4), (2012).
- [29] Yuangyai, C., Nembhard, H.B., “Emerging Nanotechnologies for Manufacturing, Micro and Technologies. Chapter 8 – Design of Experiments: A Key to Innovation in Nanotechnology,” 2010, 207 – 234. William Andrew.